Brain pathology caused in the neonatal macaque by short and prolonged exposures to anticonvulsant drugs

Kevin K. Noguchi[a], **Nicole A. Fuhler**[a], **Sophie H. Wang**[a], **Saverio Capuano III**[b], **Kevin R. Brunner**[b], **Shreya Larson**[b], **Kristin Crosno**[b], **Heather A. Simmons**[b], **Andres F. Mejia**[b], **Lauren D. Martin**[c], **Gregory A. Dissen**[d], **Ansgar Brambrink**[e], **Chrysanthy Ikonomidou**[f,*]

[a]Department of Psychiatry, Washington University, School of Medicine, St Louis, USA

[b]Wisconsin National Primate Research Center, Madison, WI, USA

[c]Division of Comparative Medicine, Oregon National Primate Research Center, Oregon Health & Science University, Beaverton, OR, USA

[d]Division of Neuroscience, Oregon National Primate Research Center, Oregon Health & Science University, Beaverton, OR, USA

[e]Department of Anesthesiology, Columbia University, New York Presbyterian Hospital, Irving Medical Center, New York, NY, USA

[f]Department of Neurology, University of Wisconsin, School of Medicine, Madison, WI, USA

Abstract

Barbiturates and benzodiazepines are potent $GABA_A$ receptor agonists and strong anticonvulsants. In the developing brain they can cause neuronal and oligodendroglia apoptosis, impair synaptogenesis, inhibit neurogenesis and trigger long-term neurocognitive sequelae. In humans, the vulnerable period is projected to extend from the third trimester of pregnancy to the third year of life.

Infants with seizures and epilepsies may receive barbiturates, benzodiazepines and their combinations for days, months or years. How exposure duration affects neuropathological sequelae is unknown. Here we investigated toxicity of phenobarbital/midazolam (Pb/M) combination in the developing nonhuman primate brain.

Neonatal rhesus monkeys received phenobarbital intravenously, followed by infusion of midazolam over 5 ($n = 4$) or 24 h (n = 4). Animals were euthanized at 8 or 36 h and brains examined immunohistochemically and stereologically.

*Corresponding author at: Department of Neurology, University of Wisconsin Madison, 1685 Highland Avenue, Madison, WI 53705, USA. Ikonomidou@neurology.wisc.edu (C. Ikonomidou).

Treatment was well tolerated, physiological parameters remained at optimal levels. Compared to naive controls, Pb/M exposed brains displayed widespread apoptosis affecting neurons and oligodendrocytes. Pattern and severity of cell death differed depending on treatment-duration, with more extensive neurodegeneration following longer exposure. At 36 h, areas of the brain not affected at 8 h displayed neuronal apoptosis, while oligodendroglia death was most prominent at 8 h. A notable feature at 36 h was degeneration of neuronal tracts and trans-neuronal death of neurons, presumably following their disconnection from degenerated presynaptic partners.

These findings demonstrate that brain toxicity of Pb/M in the neonatal primate brain becomes more severe with longer exposures and expands trans-synaptically. Impact of these sequelae on neurocognitive outcomes and the brain connectome will need to be explored.

1. Introduction

GABA (γ-aminobutyric acid) is a major inhibitory neurotransmitter in the mammalian central nervous system and regulates brain development at molecular, cellular and systems level (Daniel et al., 1998; Nicholls and Attwell, 1990; Seeburg, 1993). Barbiturates and benzodiazepines, most potent anticonvulsant and sedative drugs, positively modulate GABA$_A$ receptors to produce their desired therapeutic effects.

Two decades ago, it was reported that antagonists of the *N*-methyl-D-aspartate (NMDA) subtype of glutamate receptors and agonists at GABA$_A$ receptors (Ikonomidou et al., 1999, 2000), including numerous sedative, antiepileptic (AEDs; Bittigau et al., 2002), and general anesthetic drugs (ketamine, nitrous oxide, propofol, isoflurane, sevoflurane) (Brambrink et al., 2012a, 2012b, 2010: Creeley et al., 2010; Jevtovic-Todorovic et al., 2003; Slikker Jr et al., 2007) cause widespread apoptotic death in the developing rat brain during the brain growth spurt period. They trigger apoptosis of neurons and oligodendroglia but also suppress neurogenesis (Stefovska et al., 2008), inhibit normal synapse development and maturation (Forcelli et al., 2012; Jevtovic-Todorovic et al., 2013) and cause long-lasting behavioral and cognitive impairments in rodents and non-human primates (NHPs), if exposure occurs during the brain growth spurt period (Fredriksson et al., 2007; Stefovska et al., 2008; Paule et al., 2011). In humans, this period is projected to encompass the third trimester of pregnancy to the third year of life (Dobbing and Sands, 1979).

Retrospective clinical studies in children exposed to AEDs in utero, during infancy or early childhood have delivered evidence for a correlation between early developmental drug exposure and adverse neuro-developmental outcomes. Farwell et al. (1990) demonstrated that phenobarbital treatment of children with febrile seizures leads to long-term deficits in IQ. It has been documented in multicenter human research (Meador KJ and NEAD Study Group, 2009; Meador and NEAD Study Group, 2012) that children exposed to valproate in the 3rd trimester of pregnancy have a 9-point deficit in IQ, and those exposed to other AEDs

(carbamazepine, lamotrigine, phenytoin) have impaired verbal abilities at age 4.5 years. Brain morphology of subjects exposed in utero to AEDs has been analyzed by means of magnetic resonance imaging volumetry (Ikonomidou et al., 2007) and lower grey matter volumes in exposed subjects were reported in the lentiform nucleus, including pallidum and putamen bilaterally, and the hypothalamus. In these studies, effects of AED therapy could be separated from the effects of a disease, because the fetal brain only experienced drug exposure.

Millions of human fetuses and infants are treated with antiepileptic agents each year. The combination of high doses of phenobarbital (Pb), benzodiazepines (lorazepam, midazolam, diazepam) and other AEDs has become the accepted standard of care for medical management of prolonged, recurrent seizures and status epilepticus in infancy (Glass and Shellhaas, 2019; Soul, 2018). In addition, combinations of barbiturates, benzodiazepines and opiates are used to sedate infants with critical illnesses for days or weeks in the intensive care. While the impact of surgical anesthesia on the developing brain has and is being actively investigated at both preclinical and clinical settings, the question whether prolonged treatments with anticonvulsant and sedative drugs have deleterious effects on the developing human brain has received less attention, despite the fact that exposures to such agents are typically much longer (days, weeks and even years) than exposures to surgical anesthesia (few to several hours).

This study was designed to explore neuropathological sequelae that result from exposure of the infant nonhuman primate brain to the combination of phenobarbital and midazolam at clinically relevant doses and plasma concentrations. Phenobarbital has been and continues to be most popular for the treatment of seizures and status epileptics in human infants. Midazolam is often co-administered with phenobarbital to treat refractory seizures and/or achieve a level of sedation and amnesia in these infants that allows for maintenance of ventilatory support and performance of painful procedures. Our aim here has been to study and compare brain toxicity aspects associated with shorter (5 h) and longer (24 h) administrations of the phenobarbital/midazolam (Pb/M) combination. The hypothesis has been that a longer treatment duration will result in more severe neuronal pathology and spread to involve areas that do not become involved at shorter exposures.

2. Materials and methods

2.1. Animals

All animal procedures were approved by the Wisconsin National Primate Research Center, the Oregon National Primate Research Center and the University of Wisconsin - Madison and the Oregon Health and Science University Institutional Animal Care and Use Committees (IACUC) and were conducted in full accordance with the Public Health Service Policy on Humane Care and Use of Laboratory Animals.

Animals received a loading dose of phenobarbital (40 mg/kg) over 30 min followed by intravenous infusion of midazolam (loading dose of 0.5 mg/kg followed by 2–5 mg/kg and hour for 4.5 or 23.5 h. Midazolam infusion rate was adjusted to maintain a moderate level of sedation. Phenobarbital maintenance doses (2.5 mg/kg) were given at 6 and 18 h in the

animals surviving for 36 h, with the goal to maintain a therapeutically relevant phenobarbital plasma level over 36 h.

Normothermia ($T > 36.5\ °C$-$37.5\ °C$) was maintained using a servo-controlled warming blanket. Oxygen saturations were monitored with continuous pulse oximetry, vital signs with a cardiorespiratory monitor. Blood gases, blood glucose, electrolytes, lactate and hemoglobin were monitored on venous blood (femoral vein) at 0, 2, 4, 6, 12 and 24 h.

The control group ($n = 5$) consisted of 4–6 day old rhesus macaques who were separated from their mothers but not exposed to medications. These animals were returned to their mothers after a physical examination identical in nature to how the treatment animals were handled prior to medication administration. These animals were also euthanized and transcardially perfused. Perfusion fixation was performed with 4% paraformaldehyde in phosphate buffer by a trained pathologist according to institutional euthanasia standards.

2.2. Histopathology studies

Brains were serially sectioned in the coronal plane using a vibratome at 70 uM across the entire rostrocaudal extent and every 64th section immunolabeled for activated caspase-3 (AC3; CAT#9661 L; Cell Signaling Technology, Danvers, MA) as a marker of apoptosis. For immunolabeling, sections were first immersed in citrate buffer (pH 6.0) and subjected to heat in a pressure cooker for 10 min for antigen retrieval. They were then quenched in 3% hydrogen peroxide in absolute methanol for 10 min, immersed for 1 h in a blocking solution (2% Bovine Serum Albumin, 0.2% Dry Milk, 0.8% TX-100 in PBS), and incubated overnight at 4 °C with a 1:1000 dilution of AC3. The next morning, sections were incubated with a biotinylated secondary antibody (goat anti-rabbit; Vector Labs, Burlingame, CA), reacted with an avidin-biotin conjugate kit (ABC kit), and visualized using the chromogen VIP (Vectastatin Elite ABC kit and Vector VIP kits; Vector Labs, Burlingame, CA). The chromogenic AC3 staining method permits comprehensive quantification of cells irreversibly committed to apoptotic death and provides a permanent record of the cell death throughout the brain. This includes both cell bodies and processes that allows one to distinguish early from late stages of degeneration. Neurons and oligodendrocytes were easily distinguished by their location in white or grey matter in addition to each cell's unique morphological profile. In primate tissue, the AC3 antibody will produce non-specific staining in the nucleus of neurons but, in apoptotic cells, engulfs the entire cell including soma and processes making them easy to distinguish. Apoptotic oligodendrocytes are distinguished by their immunolabeled soma that is surrounded by a halo of particulate debris. Histological photocomposites were made using a Leica DM 4000B microscope equipped with a Leica DFC310FC camera and Surveyor software (Version 9.0.2.5, Objective Imaging, Kansasville, WI).

2.3. Analysis of neuronal and glial cell death

Immunofluorescence was also performed to identify apoptotic cells by co-labeling AC3 with antibodies that identify neurons (NeuN, EMD Millipore, Burlington, MA; MAB377, 1:100), astrocytes (GFAP, Sigma-Aldrich, St Louis, MO; G3893, 1:400), and oligodendrocytes (Myelin Basic Protein, EMD Millipore, Burlington, MA; MAB395, 1:200). Tissue was

blocked and incubated in primary antibodies as described above. Finally, tissue was immersed in appropriate secondary antibodies (Invitrogen, Carlsbad, CA; A21428, A11001, or A1106) for one hour before cover-slipping with mounting medium containing DAPI.

2.4. Quantification of apoptosis

2.4.1. Whole brain counts—Whole brain counts were performed using Stereoinvestigator Software (v 2019.1.3, MBF Bioscience, Williston, Vermont, USA) running on a Dell Precision Tower 5810 computer connected to a QImaging 2000R camera and a Labophot-2 Nikon microscope with electronically driven motorized stage. A rater, blind to treatment, traced each hemisection and stereologically quantified the number of neurons and oligodendrocytes using the unbiased optical fractionator method. This information was then used to estimate the number of apoptotic profiles per hemisphere which was multiplied by two to get total number per brain. Stereoinvestigator software was also used to generate cell plots of the regional distribution of neurons and oligodendrocytes using the meander scan option.

2.4.2. Regional counts—AC3 immunolabeled sections used for whole brain counts were also used to quantify regional apoptosis in the ventral cortex, hippocampus, and thalamus using Stereoinvestigator software meander scans. A subset of sections containing the hippocampus were used for counting all three regions. The hippocampi (including CA regions, dentate gyrus, and subiculum) on each section were outlined and all apoptotic cells counted within its borders. The ventral cortex roughly included the region ventral to the Sylvian fissure. More specifically, a line was drawn from the hippocampus to the point where the Sylvian fissure meets the insular cortex and all apoptotic profiles counted in the region ventral to this line (not including the hippocampus). The thalamus was also outlined and apoptotic cells counted within its borders. Finally, a density (apoptotic profiles per square millimeter) was calculated by dividing the total number of apoptotic profiles in each region by the total area.

2.5. Statistical analysis

Data are presented as means ± standard error of the mean (SEM). One sided ANOVA with post-hoc test for multiple comparisons was used to compare groups. Statistical analysis was performed with Prism (GraphPad Software, La Jolla, CA).

3. Results

Treatment with Pb/M was tolerated well in both Pb/M treatment groups. Vital signs, venous blood gases, lactate, hemoglobin and blood glucose remained within physiological levels (Table 1). Phenobarbital level on day 1 was drawn at 4 h and on day 2 shortly prior to euthanasia at 36 h. Plasma concentrations of phenobarbital on day 1 were 19.20 ± 9.59 μg/ml and, on day 2, 36.93 ± 6.25 μg/ml. Mean plasma level for Pb on days 1 + 2 was 32.46 ± 5.56 μg/ml.

Plasma levels for midazolam were drawn at 4 h and at 23.5 h, at the end of the midazolam infusion. Midazolam plasma levels were 2302 ± 1094 ng/ml on day 1 and 6018 ± 2379

ng/ml on day 2 of treatment. Mean level for midazolam on days 1 + 2 was 4160 ± 1401 ng/ml.

A profound apoptotic response to Pb/M was detected in the brains of the exposed infants at 8 h following the shorter 5 h Pb/M exposure period. This was most prominent in several divisions of the neocortex, especially the temporal cortex (layers II and IV) and the primary visual cortex (layers II and V) but also involved the caudate, globus pallidum, hippocampus, thalamus and diffusely the subcortical white matter (Fig. 1).

In the 36 h group, apoptotic pyramidal cells were present in the same brain regions as at 8 h, indicating that the neurodegenerative process was ongoing throughout the duration of drug exposure in these areas. AC3 positive neurons were present at higher densities in cortical regions at 36 h (Fig. 2 A&B).

Closer examination revealed Pb/M-induced apoptosis changed dependent on cortical region with neocortical regions exhibiting apoptosis in cortical layers II and IV/V. Apoptosis changed as the cortex transitioned to the allocortex with the entorhinal cortex displaying less apoptosis involving deeper layers when present. This pattern became more obvious at 36 h. Alternatively, the allocortical subiculum showed little apoptosis at 8 h that increased dramatically by 36 h in pyramidal neurons and their degenerating axons (Fig. 2).

In addition, findings consistent with Wallerian degeneration were captured within the subiculum (Fig. 2D and 3A), and areas not affected at 8 h now demonstrated degeneration. These areas include the subiculum, anterior thalamus and several pontine nuclei (Figs. 2C/D, 3A-D).

Immunohistochemistry confirmed that neurons and oligodendrocytes but not astrocytes were affected by the apoptosis process (Fig. 4).

Stereological analysis of the pattern and severity of the degenerative changes revealed that apoptosis affected both neurons and oligodendroglia almost equally at 8 h but neuronal death was much more severe at 36 h (Fig. 5). One way ANOVA revealed that treatment with Pb/M had a significant effect on apoptotic neurons [$F(2,10) = 34.77$, $P < 0.0001$], oligodendrocytes [$F(2,10) = 11.14$, $p = 0.0029$] and total profiles [$F(2,10) = 14.70$, $P = 0.0011$]. Post hoc analysis revealed that there were significantly more neurons affected by apoptosis at 36 h vs 8 h and controls. Despite exhibiting more than 17 times more neuronal apoptosis, the 8 h group was not significantly different from controls. This lack of significance is because we are examining three groups in an ANOVA and the 36 h group produces such a large amount of apoptosis compared to the other groups (over 53-fold more than controls). If we were to run a t-test between the control and 8 h groups only, we would get a significant result [$t(7) = 5.228$, $p = 0.0012$]. Interestingly, this also suggests that Pb/M produces far more neuronal apoptosis when given over extended periods. ANOVA revealed significant difference in oligodendrocyte apoptosis between groups [$F(2,10) = 11.14$, $p = 0.0029$]. Unlike neuronal apoptosis, the 36 h group actually exhibited less apoptosis than the 8 h group (Fig. 5). This suggests that as exposure continues, apoptotic oligodendroglia cells are removed but replaced at a slower pace by subsequent oligoapoptosis. Finally, apoptotic profiles (neurons + oligodendrocytes) were analyzed using an ANOVA and Tukey post-hoc revealing a

significant increase in apoptosis for both the 8 h and 36 h groups compared to controls [F(2,10) = 15.85, p = 0.0008]. (See Fig. 6.)

Statistical comparisons of regional apoptotic cell densities between the control and the Pb/M groups by means of one-way ANOVA revealed that apoptotic neuronal densities differed significantly between groups in the ventral cortex [F(2,10) = 21.65, P < 0.0002], the hippocampus [F (2,10) = 18.85, p < 0.0004] but not the thalamus [F(2,10) = 2.174, p > 0.05]. Post hoc comparisons with Tukey's test revealed that the severity of neuronal death was highest in the 36 h group in the ventral cortex and hippocampus. Trends in the thalamus did not reach significance.

Treatment with Pb/M had no significant effect on densities of apoptotic oligodendrocytes in any of the three regions analyzed. Such a finding is not surprising since we would expect few oligodendrocytes in these three grey matter regions. Significant effects were seen in the densities of total apoptotic profiles in the ventral cortex [F(2,10) = 15.68, P = 0.0008], hippocampus [F(2,10) = 14.14, P = 0.0012] and thalamus [F(2,10) = 5.323, P = 0.0267].

4. Discussion

This study was designed to explore whether the combination of a barbiturate and a benzodiazepine, at doses and plasma concentrations that are clinically relevant for the treatment of human infants, can trigger cell death in the developing nonhuman primate brain and how this injury evolves with increasing duration of the exposure. We wanted to mimic the clinical situation of administering Pb/M for recurrent seizures or status epilepticus, whereby treatment durations of 24 h and longer are encountered frequently (Glass and Shellhaas, 2019).

The key findings of our study are that

    a. Pb/M causes apoptosis of neurons and oligodendrocytes in the neonatal NHP brain at plasma concentrations relevant to the treatment of human infants;

    b. within those brain regions where neuronal apoptosis is present at 8 h, neurodegeneration markedly increases in severity after the longer exposure;

    c. oligodendroglial apoptosis demonstrates an early peak at 8 h with subsequently declining pace at 36 h;

    d. with longer exposures the neuroapoptotic process leads to degeneration of axons and expands to affect trans-neuronal targets within interconnected brain regions (subiculum, pons, anterior thalamus).

These findings suggest that longer treatments, in addition to increasing severity of neurodegeneration in most vulnerable regions, also trigger connectomic pathology through Wallerian and trans-neuronal degeneration.

The strong proapoptotic properties of $GABA_A$ agonists, which include barbiturates, benzodiazepines and many anesthetics, have been known for years. Our current understanding of the pathophysiology entails that toxicity of these drugs is initiated by

disturbances in physiologic excitatory neurotransmission. At early developmental stages of ongoing physiological programmed cell death in the brain, aiming to actively eliminate unnecessary cells, synaptic activity critically controls intracellular survival pathways and related gene transcription in neurons and immature oligodendrocytes. Pathomechanisms implicated include reduction in synthesis of neurotrophins, reduced levels of the active phosphorylated forms of extracellular signal regulated kinase (ERK1/2) and protein kinase B (AKT) which suppress the intrinsic apoptotic pathway (Bittigau et al., 2002; Hansen et al., 2004). The cell death process is Bax-dependent (Young et al., 2003) and involves down regulation of $BClx_L$, mitochondrial injury and extra-mitochondrial leakage of cytochrome c (Hansen et al., 2004; Yon et al., 2005). This is followed by a sequence of changes culminating in activation of caspase 3 (Olney et al., 2001, 2002). Involvement of reactive oxygen species and oxidative stress in the pathogenesis of this phenomenon has been suggested as well (Léveillé et al., 2010; Papadia et al., 2008). Studies using microarray analysis of rat brains exposed to anesthetics revealed differential expression of many genes involved in multiple pathways directly related to brain function, the significance of which remains to be explored (Liu et al., 2013). Similarly, analysis of the brain proteome of mice exposed to NMDA antagonists or $GABA_A$ agonists demonstrated long-term dysregulation of proteins associated with apoptosis, oxidative stress, inflammation, cell proliferation and neuronal circuit formation (Kaindl et al., 2008). This is in accordance with reports that anesthetics and antiepileptics lead to a persistent decrease of synapses in several brain regions in rodents and suppress neurogenesis (Forcelli et al., 2012; Jevtovic-Todorovic et al., 2013; Stefovska et al., 2008). More recent work in nonhuman primates also implicates involvement of glial activation which may serve as a surrogate marker for neurotoxicity (Zhang et al., 2016).

Whether these same mechanisms that have been described in rodents apply to the primate brain has not been investigated. Interestingly, lithium, a strong activator of ERK1/2, abolishes neurotoxicity of anesthetics and ethanol in rodents (Straiko et al., 2009; Young et al., 2008) and isoflurane in the infant nonhuman primate brain (Noguchi et al., 2016), suggesting that pathomechanisms may indeed be similar among species.

Since the discovery of neurotoxicity and gliotoxicity of GABAmimetics in mammals, the question has been posed as to the clinical relevance of this phenomenon. Studies performed in rodents have suggested that doses and plasma levels required to cause apoptosis are likely relevant to humans (Bittigau et al., 2002). We now provide direct evidence in a primate species, by demonstrating pro-apoptotic effect of two $GABA_A$ mimetics, phenobarbital and midazolam, at doses and plasma levels that are clinically relevant for the treatment of human infants. Phenobarbital continues to be most popular as a first line anticonvulsant for neonatal and infantile seizures with target plasma levels in the range of 20–40 μg/ml. Midazolam is added to phenobarbital for the treatment of intractable seizures and administered in humans as a continuous infusion at rates of up to 0.5 mg/kg/h (Glass and Shellhaas, 2019). Achieved midazolam plasma concentration in infants have not been well studied, but available data from neonates on ECMO treated with midazolam infusions have revealed plasma levels of up to 4 μg/ml (4000 ng/ml) within 48 h, at an infusion rate of 0.25 mg/kg/h (Mulla et al., 2003). The midazolam and phenobarbital plasma levels measured in the NHP neonates in our study (2302 ± 1094 ng/ml on day 1 and 6018 ± 2379 ng/ml on day 2 for midazolam;

19.20 ± 9.59 μg/ml on day 1 and 36.93 ± 6.25 μg/ml on day 2 for phenobarbital) are comparable to levels measured in human infants treated with these same medications. Our data strongly suggest that the combined treatment of human infants with Pb/M, as currently practiced in neonatal and pediatric intensive care units, bears the potential to cause brain injury.

There is a continuing discussion as to whether $GABA_A$ agonists and NMDA antagonists may simply accelerate physiological apoptosis without causing additional cell loss. Our data strongly argue against this hypothesis, especially for neurons, as they show that, within the most vulnerable brain regions, i.e. the ones that demonstrated neurodegeneration at 8 h, longer exposures to Pb/M resulted in significantly higher numbers of apoptotic neurons. From previous work in mice exposed to ethanol we know that AC3 positivity of apoptotic cells is a transient phenomenon, likely transpires within 2–3 h for a given neuron and within 6–8 h for a group of like-type neurons, following which cell fragments are removed and undetectable (Olney et al., 2002). This implies that the AC3 positive neurons detected at 36 h were different from the ones detected at 8 h, that multiple death cycles had already taken place and that, as time passed, the pace of neuronal death markedly accelerated. At 8 h we estimated a 17-fold increase and at 36 h a 54-fold increase in neuroapoptosis. Given that we only examined the brains at 2 time points, the true extent of neuronal cell loss during the 36 h remains unknown.

Searching for explanation for apoptosis acceleration with time, we hypothesize that the most vulnerable, likely least networked neurons, succumbed first, while the more robust ones managed to maintain their trophic support above a critical level for a while. Eventually, further progressive weakening of local excitatory circuits due to prolonged synaptic effects of the drugs, on one hand, and degeneration of their local and/or distant synaptic partners on the other, initiated the apoptosis cascade in those neurons that would have survived a shorter exposure.

We similarly need to consider the transient nature of AC3 immunopositivity when interpreting oligoapoptosis, since the 8 h group exhibited more apoptosis than the 36 h group. At 8 h we estimated a 5-fold increase and at 36 h a 2.4-fold increase in oligoapoptosis. Rather than prolonged exposure reducing oligoapoptosis, it is far more likely that the initial apoptotic surge was replaced by a smaller number of degenerating oligodendrocytes.

Our data further demonstrate that Pb/M-induced degeneration triggers axonal Wallerian degeneration and trans-neuronal apoptosis attributable to de-afferentiation and/or de-efferentiation. At 36 h we found trans-neuronal degeneration occurring in the pons, anterior thalamus, and subiculum. While the only evidence of Wallerian degeneration captured at 36 h was seen in subicular pyramidal axons, the true extent of this process is likely greatly underestimated based on the data available so far. According to research in different mammalian species, this type of axonal pathology begins within 24 h in rodents but can take several days in primates (Vargas and Barres, 2007). Hence, we hypothesize that we only captured the early onset of this process in the NHP brains we examined. Similar patterns of trans-neuronal apoptotic degeneration have been described after traumatic brain injury in the

neonatal mouse (Bayly et al., 2006; Bittigau et al., 1999). After concussive blows to the head, apoptosis was seen in the frontal, parietal, cingulate and retrosplenial cortices, thalamic nuclei, dentate gyrus, caudate nucleus and subiculum followed by delayed apoptosis in the mammillary bodies. It was suggested that the initial anterior thalamic apoptosis resulted in trans-neuronal degeneration in the mammillary bodies, which fits with other studies showing that mammillary bodies are susceptible to trans-neuronal apoptosis (Ginsberg and Martin, 2002). Similarly, others have found that pyramidal tract lesions produce trans-neuronal degeneration in the pons in animals (Trumpy, 1971) and humans (Wakamoto et al., 2006) that is heightened during development. Connectomic vulnerability may also explain why pontosubicular degeneration is commonly reported following perinatal death and seen following a wide variety of insults, particularly following white matter injury (Burke and Gobe, 2005).

In conclusion, we are showing that the combinations of a barbiturate and a benzodiazepine, at clinically relevant doses and plasma concentrations, causes both somal apoptosis and connectomic pathology in the neonatal NHP brain. Severity of neurodegeneration increases with duration of exposure. Ongoing behavioral studies in NHP survivors will help determine whether these neuropathological sequelae result in deficits in social behaviors and cognitive function.

Acknowledgements

References

Bayly PV, Dikranian KT, Black EE, et al., 2006 Spatiotemporal evolution of apoptotic neurodegeneration following traumatic injury to the developing rat brain. Brain Res. 1107, 70–81. [PubMed: 16822489]

Bittigau P, Siiringer M, Pohl D, et al., 1999 Apoptotic neurodegeneration following trauma is markedly enhanced in the immature brain. Ann. Neurol 45, 724–735. [PubMed: 10360764]

Bittigau P, Sifringer M, Genz K, et al., 2002 Antiepileptic drugs and apoptotic neurodegeneration in the developing brain. Proc. Natl. Acad. Sci 99, 15089–15094. [PubMed: 12417760]

Brambrink AM, Evers AS, Avidan MS, et al., 2010 Isoflurane-induced neuroapoptosis in the neonatal rhesus macaque brain. Anesthesiology 112 (834–141). [PubMed: 20234312]

Brambrink AM, Back SA, Riddle A, et al., 2012a Isoflurane-induced apoptosis of oligodendrocytes in the neonatal primate brain. Ann. Neurol 2, 525–535.

Brambrink AM, Evers AS, Avidan MS, et al., 2012b Ketamine-induced neuroapoptosis in the fetal and neonatal rhesus macaque brain. Anesthesiology 116, 372–384. [PubMed: 22222480]

Burke C, Gobe G, 2005 Pontosubicular apoptosis ('necrosis') in human neonates with intrauterine growth retardation and placental infarction. Virchows Arch. 446, 640–645. [PubMed: 15838644]

Creeley CE, Dikranian KT, Dissen GA, et al., 2010 Propofol-induced apoptosis of neurons and oligodendrocytes in the fetal and neonatal rhesus macaque brain. Br. J. Anaesth 10, i29–i38.

Daniel H, Levenes C, Crepel F, 1998 Cellular mechanisms of cerebellar LTD. Trends Neurosci. 21, 401–407. [PubMed: 9735948]

Dobbing J, Sands J, 1979 The brain growth spurt in various mammalian species. Early Hum. Dev 3, 79–84. [PubMed: 118862]

Farwell JR, Lee YJ, Hirtz DG, et al., 1990 Phenobarbital for febrile seizures - effects on intelligence and on seizure recurrence. N. Engl. J. Med 322, 364–369. [PubMed: 2242106]

Forcelli PA, Janssen MJ, Vicini S, Gale K, 2012 Neonatal exposure to antiepileptic drugs disrupts striatal synaptic development. Ann. Neurol 72, 363–372. [PubMed: 22581672]

Fredriksson A, Ponten E, Gordh T, Eriksson P, 2007 Neonatal exposure to a combination of N-methyl-d-aspartate and γ-aminobutyric acid type a receptor anesthetic agents potentiates apoptotic neurodegeneration and persistent behavioral deficits. Anesthesiology 107, 427–436. [PubMed: 17721245]

Ginsberg SD, Martin LJ, 2002 Axonal transection in adult rat brain induces transsynaptic apoptosis and persistent atrophy of target neurons. J. Neurotrauma 19, 99–109. [PubMed: 11852982]

Glass HC, Shellhaas RA, 2019 Acute symptomatic seizures in neonates. Semin. Pediatr. Neurol 32, 100768 10.1016/j.spen.2019.08.004. [PubMed: 31813514]

Hansen HH, Briem T, Dzietko M, et al., 2004 Mechanisms leading to disseminated apoptosis following NMDA receptor blockade in the developing rat brain. Neurobiol. Dis 16, 440–453. [PubMed: 15193300]

Ikonomidou C, Bosch F, Miksa M, et al., 1999 Blockade of NMDA receptors and apoptotic neurodegeneration in the developing brain. Science 283, 70–74. [PubMed: 9872743]

Ikonomidou C, Bittigau P, Ishimaru MJ, et al., 2000 Ethanol-induced apoptotic neurodegeneration and fetal alcohol syndrome. Science 287, 1056–1060. [PubMed: 10669420]

Ikonomidou C, Scheer I, Wilhelm T, et al., 2007 Brain morphology alterations in the basal ganglia and the hypothalamus following prenatal exposure to antiepileptic drugs. Eur. J. Paediatr. Neurol 11, 297–301. [PubMed: 17418601]

Jevtovic-Todorovic V, Hartman RE, Izumi Y, et al., 2003 Early exposure to common anesthetics causes widespread neurodegeneration in the developing rat brain and persistent learning deficits. J. Neurosci 23, 876–882. [PubMed: 12574416]

Jevtovic-Todorovic V, Absalom AR, Blomgren K, et al., 2013 Anaesthetic neurotoxicity and neuroplasticity: an expert group report and statement based on the BJA Salzburg seminar. Br. J. Anaesth 111, 143–151. [PubMed: 23722106]

Kaindl AM, Koppelstaetter A, Nebrich G, et al., 2008 Brief alteration of NMDA or GABAA receptor-mediated neurotransmission has long term effects on the developing cerebral cortex. Mol. Cell. Proteomics 7 (229302310).

Léveillé F, Papadia S, Fricker M, et al., 2010 Suppression of the intrinsic apoptosis pathway by synaptic activity. J. Neurosci 30, 2623–2635. [PubMed: 20164347]

Liu F, Guo L, Zhang J, et al., 2013 Inhalation anesthesia-induced neuronal damage and gene expression changes in developing rat brain. Sys. Pharmacol 1, 1–9.

Meador KJ and NEAD Study Group, 2009 Cognitive function at 3 years of age after fetal exposure to antiepileptic drugs. N. Engl. J. Med 360, 1597–1605. [PubMed: 19369666]

Meador KJ, NEAD Study Group, 2012 Effects of fetal antiepileptic drug exposure: outcomes at age 4.5 years. Neurology 78, 1207–1214. [PubMed: 22491865]

Mulla H, McCormach P, Lawson G, Firmin RK, Upton DR, 2003 Pharmacokinetics of midazolam in neonates undergoing extracorporeal membrane oxygenation. Anesthesiology 99, 275–282. [PubMed: 12883399]

Nicholls D, Attwell D, 1990 The release and uptake of excitatory amino acids. Trends Pharmacol. Sci 11, 462–468. [PubMed: 1980041]

Noguchi KK, Johnson SA, Kristich LE, et al., 2016 Lithium protects against anaesthesia neurotoxicity in the infant primate brain. Sci. Rep 6, 22427 10.1038/strep22427. [PubMed: 26951756]

Olney JW, Tenkova T, Dikranian K, et al., 2001 Ethanol-induced apoptotic neurodegeneration in the developing C57BL/6 mouse brain. Dev. Brain Res 133, 115–126.

Olney JW, Tenkova T, Dikranian K, et al., 2002 Ethanol-induced caspase- 3 activation in the in vivo developing mouse brain. Neurobiol. Dis 9, 205–219. [PubMed: 11895372]

Papadia S, Soriano FX, Léveillé F, et al., 2008 Synaptic NMDA receptor activity boosts intrinsic antioxidant defences. Nat. Neurosci 11, 476–487. [PubMed: 18344994]

Paule MG, Li M, Zou X, Hotchkiss C, et al., 2011 Ketamine anesthesia during the first week of life can cause long-lasting cognitive deficits in rhesus monkeys. Neurotoxicol. Teratol 33, 220–230. [PubMed: 21241795]

Seeburg PH, 1993 The TINS/TIPS lecture: the molecular biology of mammalian glutamate receptor channels. Trends Neurol. Sci 16, 359–365.

Slikker W Jr., Zou X, Hotchkiss CE, et al., 2007 Ketamine-induced neuronal cell death in the perinatal rhesus monkey. Toxicol. Sci 98, 145–158. [PubMed: 17426105]

Soul JS, 2018 Acute symptomatic seizures in term neonates: etiologies and treatments. Semin. Fetal Neonatal Med 23, 183–190. [PubMed: 29433814]

Stefovska V, Czuczwar M, Smitka M, et al., 2008 Sedative and anticonvulsant drugs suppress postnatal neurogenesis. Ann. Neurol 64, 434–445. [PubMed: 18991352]

Straiko MMW, Young C, Cattano D, et al., 2009 Lithium protects against anesthesia-induced developmental neuroapoptosis. Anesthesiology 110, 862–868. [PubMed: 19293695]

Trumpy JH, 1971 Transneuronal degeneration in the pontine nuclei of the cat. I. Neuronal changes in animals of varying ages. II. The glial proliferation. Ergeb Anat Entwicklungsgesch 44, 3–72.

Vargas ME, Barres BE, 2007 Why is Wallerian degeneration in the CNS so slow? Annu. Rev. Neurosci 30, 153–179. [PubMed: 17506644]

Wakamoto H, Eluvathingal TJ, Makki M, Juhász C, Chugani HT, 2006 Diffusion tensor imaging of the corticospinal tract following cerebral hemispherectomy. J. Child Neurol 21, 566–571. [PubMed: 16970845]

Yon JH, Daniel-Johnson J, Carter LB, Jevtovic-Todorovic V, 2005 Anesthesia induces suicide in the developing rat brain via the intrinsic and extrinsic apoptotic pathways. Neuroscience 135, 815–827. [PubMed: 16154281]

Young C, Klocke BJ, Tenkova T, et al., 2003 Ethanol induced neuronal apoptosis in the in vivo developing mouse brain is BAX dependent. Cell Death Differ. 10, 1148–1155. [PubMed: 14502238]

Young C, Straiko MMW, Johnson SA, Creeley C, Olney JW, 2008 Ethanol causes and lithium prevents neuroapoptosis and suppression of pERK in the infant mouse brain. Neurobiol. Dis 31, 355–360. [PubMed: 18595723]

Zhang X, Liu S, Newport GD, et al., 2016 In vivo monitoring of sevoflurane-induced adverse effects in neonatal nonhuman primates using small-animal positron emission tomography. Anesthesiology 125, 133–146. [PubMed: 27183169]
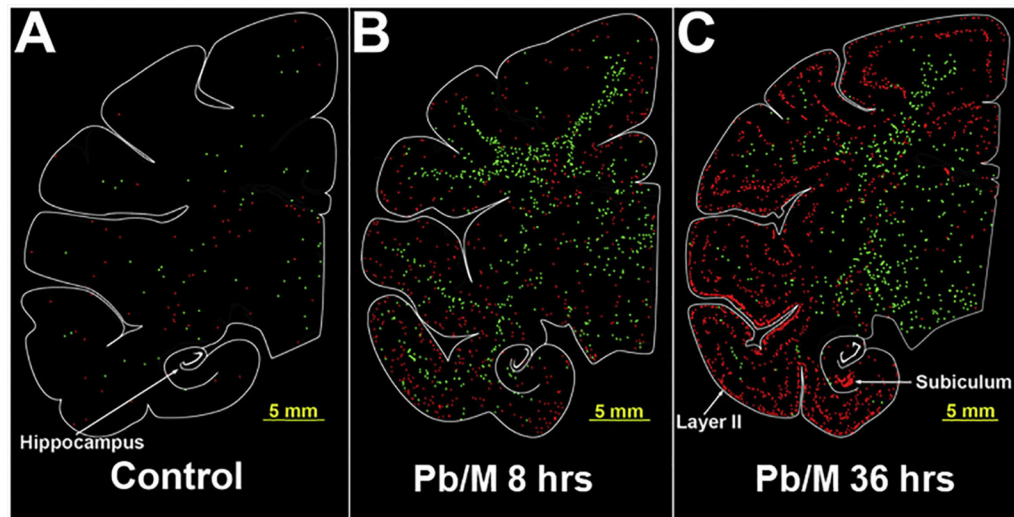
Fig. 1.
Apoptosis in the neonatal rhesus macaque brain following Pb/M exposure. A - C show computer generated plots of neuroapoptosis (red dots) and oligoapoptosis (green dots) in the brains of a rhesus control infant macaque (A), an infant exposed to Pb/M for 5 h and euthanized at 8 h (B) and an infant exposed to Pb/M for 24 h and euthanized at 36 h (C). There is substantial amount of neuro- and oligoapoptosis in the brains of both treated animals. At this level and at both time points there is homogeneous pattern of neuro and oligoapoptosis in the caudate, extending into the thalamus, hypothalamus, corpus callosum and subcortical white matter. A laminar pattern of neuronal apoptosis appears within the cingulate, frontal somatosensory, insular, temporal, entorhinal cortices and subiculum. Note the much denser neuroapoptosis pattern within the cortical areas at 36 h. Cell plots of control animals show low levels of physiological apoptosis. Scale bar = 5 mm.
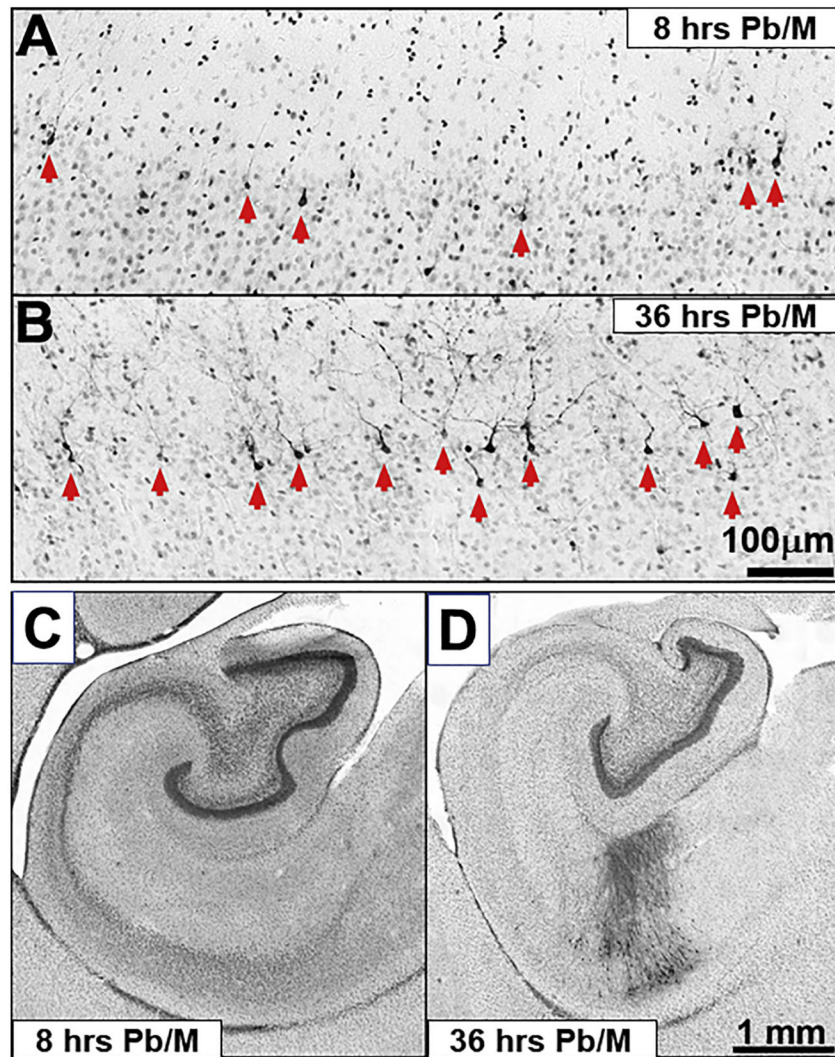
Fig. 2.
Light micrographs depicting AC3 positive profiles (red arrows) within the temporal cortex in a rhesus monkey exposed to Pb/M and euthanized at 8 h (A) and a monkey exposed to the drug combination for 24 h and euthanized at 36 h. Note that AC3 immuno-positive neurons are present at higher density in the cortex and that neuronal processes are more prominently stained at 36 h. C and D show low power micrographs of the hippocampus with AC3 positive staining of pyramidal cells and their axons in the subiculum. Bar in A & B 100 μm; Bar in C & D 1 mm.
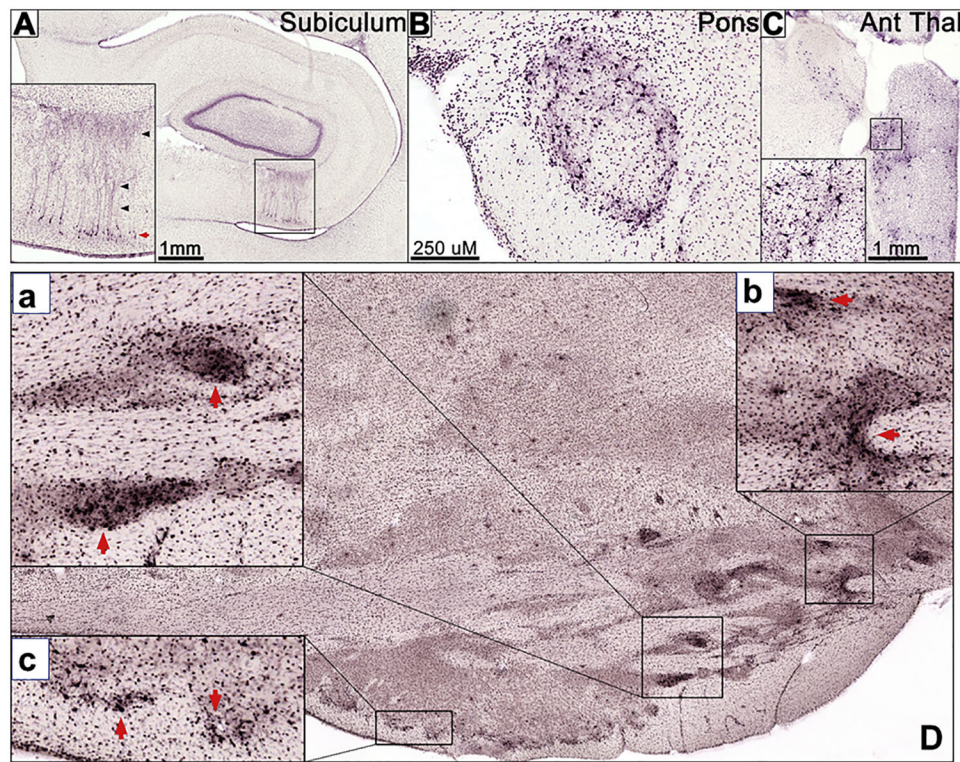
Fig. 3.

Prolonged Phenobarbital/Midazolam exposure produces connectomic pathology in the subiculum (A), pons (B & D), and anterior thalamus (C) of the neonatal macaque. A P6 neonatal macaque was administered Pb/M over 24 h and euthanized at 36 h. [A] Apoptotic (AC3 immunopositive) pyramidal cells are found in the subiculum (red arrows) along with Wallerian degeneration in axons (black arrows). Apoptosis was also present in the caudal pons [B, D] and anterior thalamus (Ant Thal) [C]. The magnified views a-c in D depict AC3 immuno-positive pontine nuclei.
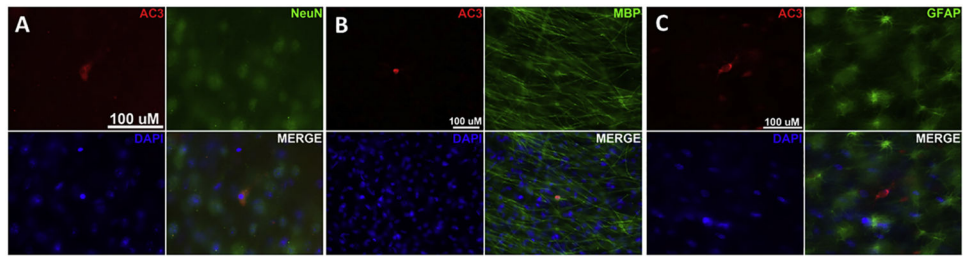
Fig. 4.

Composites A-C show confocal images of NeuN, MBP, GFAP, AC3 and DAPI stained sections. There is colocalization of NeuN with AC3 and MBP with AC3 indicating neuronal and oligodendroglia apoptosis respectively. In C, GFAP staining (green) does not colocalize with AC3 (red) indicating that astroglia are not affected by the proapoptotic effect of Pb/M.
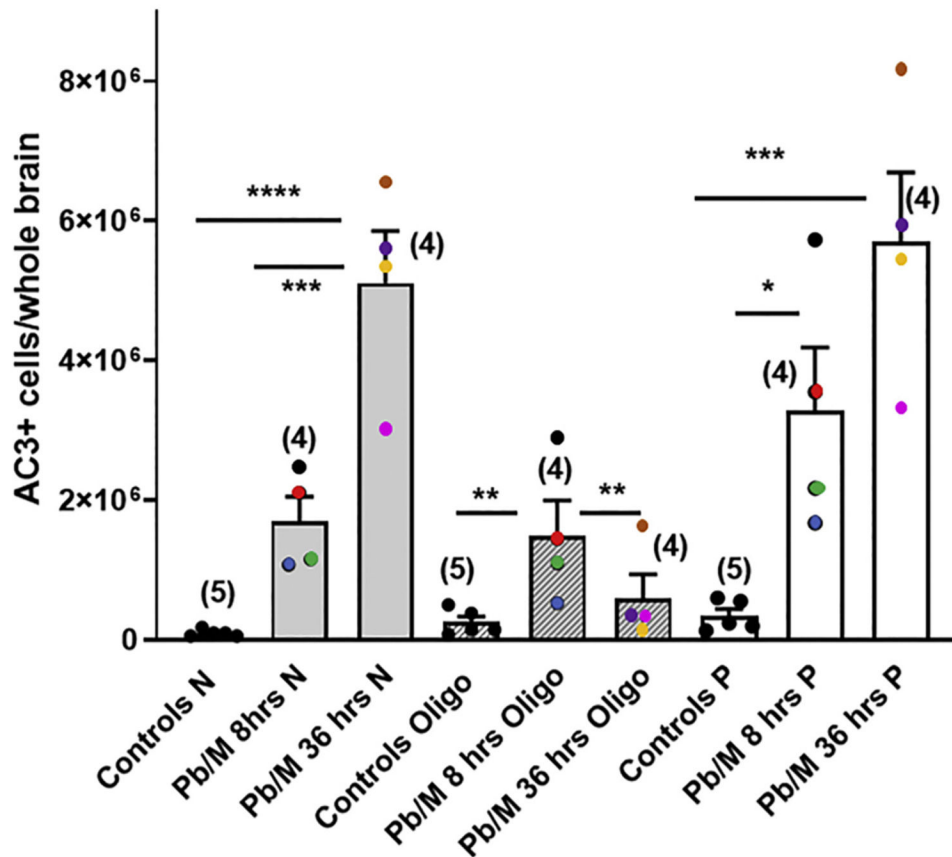
Fig. 5.
Pb/M induces widespread apoptosis in the infant macaque brain affecting neurons and oligodendrocytes, at both 8 and 36 h. The graphs illustrate numbers of apoptotic neurons (black), apoptotic oligodendrocytes (grey) and apoptotic profiles (white) counted in the brains of control neonatal macaques ($n = 5$) and infants treated with Pb/M and euthanized at 8 ($n = 4$) or 36 h (n = 4). Controls are animals not exposed to drugs. Columns represent means ± SEM of total numbers of neurons (N; grey), oligodendrocytes (Oligo; shaded) and total apoptotic profiles (white), counted in the whole brain. Dots represent individual animals and same color dots depict counts from the same animal. Statistical comparisons between the control and the Pb/M groups were performed by means of one-way ANOVA with post hoc Tukey's test (*$P < 0.05$; **$P < 0.01$; ***$P < 0.001$; ****$P < 0.0001$).
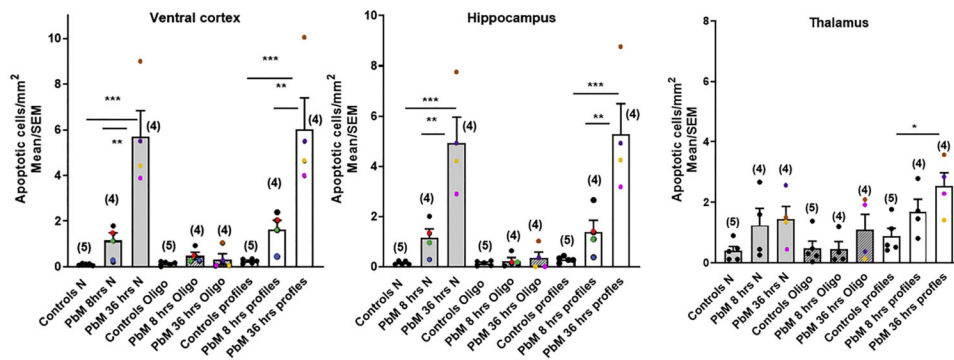
Fig. 6.

Effects of Pb/M at 8 and 36 hrs on apoptosis of neurons (N), oligodendrocytes (Oligo) and total profiles (N+Oligo) in the ventral cortex, hippocampus and thalamus. Within the ventral cortex and the hippocampus, Pb/M exposure had a significant effect on neuronal apoptosis (black columns) and total profiles (white) but not on oligoapoptosis (grey columns). Neuronal apoptosis was significantly more severe at 36 hrs in both brain regions. The effects on apoptosis in the thalamus only reached significance at 36 hrs for total profiles densities, although trends were evident for neurons as well.

Columns represent means ± SEM of densities (cells per square millimeter) of total apoptotic profiles (white), neurons (black) and oligodendrocytes (Oligos; grey). Dots represent individual animals and same color dots depict counts from the same animal. Numbers in parentheses represent numbers of animals in each group. Stars represent the level of significance between respective groups based on post hoc analysis with the Tukey's test; $*P < 0.05$; $**P < 0.01$; $***P < 0.001$

Table 1

Physiologic variables in infant rhesus monkeys subjected to Pb/M for 5 or 24 h. Animals in group 1 were euthanized at 8 h and in group 2 at 36 h. Measurements were taken at 0.5, 2, 4, 6, 12 and 24 h after initiation of Pb injection and represent means ± SEM. All values are within physiological range. HR: heart rate; pCO_2: partial CO_2 pressure; SaO_2: oxygen saturation measured by pulse oximetry; Hb: hemoglobin.

	Weight (kg) (mean ± SEM)	Age (days) (mean ± SEM)	Sex distribution	0.5 h (mean ± SEM)	2 h (mean ± SEM)	4 h (mean ± SEM)	6 h (mean ± SEM)	12 h (mean ± SEM)	24 h (mean ± SEM)
Pb/M 5 h (n = 4)	0.43 ± 0.04	5.25 ± 0.48	4F, 0 M						
pH (venous)				7.327 ± 0.034	7.349 ± 0.019	7.327 ± 0.035	7.359 ± 0.021		
HR (beats/min)				268.30 ± 17.85	186.80 ± 15.85	182.00 ± 12.49	182.30 ± 16.50		
pCO_2 (mmHg)				51.23 ± 4.66	48.33 ± 3.34	49.08 ± 7.47	44.10 ± 4.76		
SaO_2 (%)				98.00 ± 2.00	98.50 ± 0.65	99.00 ± 0.71	99.00 ± 0.25		
Lactate (mM)				1.39 ± 0.54	1.11 ± 0.19	1.13 ± 0.29	1.09 ± 0.25		
Hb (mg/dl)				13.35 ± 2.16	12.90 ± 2.11	12.25 ± 2.35	11.45 ± 2.10		
Glucose (mM)				69.00 ± 9.86	56.25 ± 8.90	50.75 ± 4.52	42.50 ± 7.86		
Pb/M 24 h; (n= 4)	0.48 ± 0.05	5.75 ± 1.60	2 M, 2F						
pH (venous)				7.332 ± 0.030	7.354 ± 0.020	7.383 ± 0.021	7.360 ± 0.001	7.338 ± 0.024	7.286 ± 0.016
HR (beats/min)				214.50 ± 6.30	197.50 ± 9.82	186.00 ± 6.67	187.00 ± 3.76	197.00 ± 7.38	180.80 ± 13.40
pCO_2 (mmHg)				48.9 ± 4.90	44.75 ± 3.45	48.85 ± 3.91	43.28 ± 1.90	37.53 ± 0.70	42.58 ± 3.88
SaO_2 (%)				97.99 ± 2.12	97.00 ± 1.92	97.00 ± 1.09	96.50 ± 1.32	97.50 ± 1.50	98.25 ± 1.03
Lactate (mM)				3.54 ± 0.98	2.17 ± 0.65	1.08 ± 0.11	1.15 ± 0.06	1.32 ± 0.29	1.31 ± 0.34
Hb (mg/dl)				14.55 ± 1.40	13.38 ± 0.32	13.68 ± 1.33	13.85 ± 0.93	11.80 ± 0.84	12.35 ± 0.57
Glucose (mM)				65.00 ± 3.08	57.25 ± 3.97	42.00 ± 2.80	43.00 ± 1.47	41.25 ± 6.59	60.75 ± 21.09